Deformation and degradation behaviour of Rubber Intermixed Ballast System under cyclic loading

Chathuri M. K. Arachchige
BSc (Hons)
PhD Candidate, Transport Research Centre, School of Civil and Environmental Engineering, University of Technology Sydney, NSW 2007. Australia.
Email: chathuri.arachchige@student.uts.edu.au
ORCID ID: https://orcid.org/0000-0003-1554-6527

Buddhima Indraratna
PhD (Alberta), MSc (Lond.), BSc (Hons., Lond.), DIC, FTSE, FIEAust., FGS, CEng, CPEng
Distinguished Professor of Civil Engineering, Founding Director of Australian Research Council's Industrial Transformation Training Centre for Advanced Technologies in Rail Track Infrastructure (ITTC-Rail), Director of Transport Research Centre, School of Civil and Environmental Engineering, University of Technology Sydney, NSW 2007, Australia. Email: buddhima.indraratna@uts.edu.au
ORCID ID: https://orcid.org/0000-0002-9057-1514

Yujie Qi
PhD, MSc, BSc
Lecturer, and Program Co-leader of Transport Research Centre, School of Civil and Environmental Engineering, University of Technology Sydney, NSW 2007, Australia. Email: yujie.qi@uts.edu.au
ORCID ID: https://orcid.org/0000-0002-3486-2130

Jayan S. Vinod
PhD, M.Tech, B.Tech
Associate Professor, ARC Training Centre for Advanced Technologies in Rail Track Infrastructure (ITTC-Rail), University of Wollongong Australia, NSW 2522, Australia.
Email**:** vinod@uow.edu.au
ORCID ID: https://orcid.org/0000-0002-2611-3594

Cholachat Rujikiatkamjorn
PhD, MEng (AIT), BEng (Hons)
Professor, Transport Research Centre, School of Civil and Environmental Engineering, University of Technology Sydney, NSW 2007, Australia. Email: cholachat.rujikiatkamjorn@uts.edu.au
ORCID ID: https://orcid.org/0000-0001-8625-2839

*Author for correspondence:
Distinguished Prof. Buddhima Indraratna
School of Civil and Environmental Engineering,
Faculty of Engineering and Information Technology,
University of Technology Sydney,
Sydney NSW 2007, AUSTRALIA

Ph: +61 2 4221 3046, Email: buddhima.indraratna@uts.edu.au

ABSTRACT

In recent years, there has been an increasing interest in the use of rubber aggregates derived from waste tyres in order to improve track performance, and Rubber Intermixed Ballast System (RIBS) demonstrated some of the important geotechnical properties that reduce ballast deterioration by partially replacing ballast particles using rubber granules ranging from 9.5 to 19.5 mm. This paper focuses on evaluating the characteristics of RIBS subjected to cyclic loads by conducting large-scale triaxial tests for changing rubber contents (0-15% by weight) under confining pressures (30-60 kPa) and a loading frequency of 20 Hz following a monotonic conditioning phase. The results indicate that irreversible rearrangement of grain configurations was pronounced in RIBS with increased rubber at the conditioning phase leading to a reduction in particle deformation during the cyclic loading. It was also demonstrated that the increased rubber content in RIBS increases the energy absorption capacity and damping properties, reduces ballast breakage and resilient modulus. In addition, the study confirmed 10% by weight as the optimum rubber content in RIBS, considering the overall deformation and degradation performance of ballast.

Keywords: Tyre derived aggregates, Rubber intermixed ballast, Triaxial test, Cyclic loading, Ballast breakage, Deformation

1. Introduction

It is well known that the cyclic loads induced by trains cause ballast degradation leading to irrecoverable deformation of the track. In addition, during train loading, ballast deteriorates and accumulates fine particles due to the abrasion of ballast, breakage of angular corners and sharp edges resulting in ballast fouling. It is now well established from a variety of studies that the use of rubber inclusions (i.e., rail pads, under sleeper pads, under ballast mats, capping/ballast material modified with rubber aggregates) help in reducing ballast degradation (Remennikov et al. 2006; Jayasuriya et al. 2019; Navaratnarajah et al. 2018; Qi and Indraratna 2021; Tawk et al. 2021). In particular, some recent past studies (e.g., Fathali et al. 2016; Song et al. 2019; Esmaeili et al. 2018; Sol-Sanchez et al. 2015) have concentrated on the role of tyre derived rubber granules in ballast layer to reduce train induced surface vibrations and to control deformation and breakage by improving damping and resiliency. Koohmishi and Azarhoosh (2020) conducted tests for hydraulic conductivity of ballast and crumb rubber mixtures by changing the crumb rubber size (2-25 mm) and the percentage of rubber in the mix (0-30% by volume). They concluded that adding crumb rubber would reduce the hydraulic conductivity, but rubber-ballast mixtures could

still satisfy the required permeability even under very high rubber contents (ballast with 30% of fine-grained crumb rubber).

In Australia, over 50 million tyres reached the end of life every year, but only 69% are destined for recycling and energy recovery (Tyre Stewardship Australia 2020). Unfortunately, the rest of the tyres are still landfilled, stockpiled, or illegally dumped. There are serious environmental, social and economic hazards associated with this waste tyre disposal management. Spontaneous fires that occasionally occur in contaminated stockpiles under extreme temperatures release toxic gases (Sidhu et al. 2006; DEQ1989). Improperly discarded tyres on landfills are ideal breeding habitats for mosquitoes and rodents. Thus, recycling and reuse of rubber waste are very essential and the use of waste tyre derived rubber aggregates in ballast matrix can contribute to the widespread use of waste rubber in civil engineering applications.

Recently laboratory research studies were conducted to understand the behaviour of ballast mixed with tyre derived rubber aggregates using ballast box test apparatus (Fathali et al. 2016; Sol-Sanchez et al. 2015), direct shear test apparatus (Song et al. 2019; Gong et al. 2019), modal shaker (Esmaeili et al. 2016) and impact load test (Koohmishi and Azarhoosh, 2021). Generally, all the studies except Sol-Sanchez et al. (2015), and Koohmishi and Azarhoosh (2021), followed the similar particle size distribution of ballast for rubber granules in the mixture. Sol-Sanchez et al. (2015) added rubber crumbs in between 8-24 mm into the ballast matrix, hence the particle size distribution of granular mix deviated from the followed European ballast standard (BS EN 13450). Koohmishi and Azarhoosh (2021) conducted impact load tests for ballast following AREMA (2010) recommendations with crumb rubber in two specific size ranges of 4.75–9.5 mm and 12.5–25 mm. Generally, all these studies (e.g., Sol-Sanchez et al. 2015; Esmaeili et al. 2016; Fathali et al. 2016) explored tyre-derived aggregates mixed with ballast particles to reduce ballast degradation and stiffness while increasing the dissipated energy and damping ratio. Moreover, it has been identified that even a small increase of confining pressure (σ'_3=30-60 kPa) has a significant impact on permanent deformation of ballast under cyclic loads (Thakur et al. 2013), but the previous studies on ballast mixed with tyre-derived aggregates, however, have not been considered the changing confining pressures.

Rubber Intermixed Ballast System (RIBS) introduces blending rubber granules and ballast particles. Previous results (Lee et al. 2007) have shown that when the rubber grain size is comparatively smaller and the volume percentage of rubber is < 20%, there is only a secondary effect on the stiffness. This is because the larger particles which consist of natural rock aggregates form the load-bearing skeleton. On the other hand, if the relative size of rubber is comparatively larger, the inclusion of rubber 10-20% by volume contributes to arching in the vertical

direction and increases lateral confinement (Kim and Santamarina, 2008). This means the relative size of rubber in relation to the rock aggregates controls the load transfer mechanism, changing the macroscale behaviour. Perez et al. (2016) explains that the magnitude of deviator stress is influenced by the amount of rubber and the size of rubber granules because the rubber particle size contributes to each type of contact, i.e., rock-rubber, rock-rock and rubber-rubber contacts. The authors have proposed the particle size of rubber granules to be between 9.5 mm to 19.5 mm as a replacement to the same size of ballast particles according to the 60-graded specifications of the current Australian Standard for ballast (2758.7: 2015). The particle size distribution of proposed materials (i.e. rubber granules and RIBS) is shown in Fig. 1. The coefficient of uniformity (C_u) and the coefficient of gradation (C_c) of RIBS are 2.6 and 1.4 respectively. Large-scale triaxial testing under monotonic loading carried out on RIBS with different percentages of rubber indicates that 10% by weight is the optimum rubber content that provides a desirable shear strength, reduced dilation and controlled ballast breakage, in accordance with improved energy absorption capacity (Arachchige et al. 2021).

This study, therefore, was focused on assessing the effect of cyclic loading on RIBS in terms of degradation and deformation behaviour together with the damping properties. Evaluating and recognising the predetermined optimum rubber content (10% by weight) in the RIBS mixture is another potential concern of this study.

2. Testing program

Unlike the ballast box test and direct shear test used in the previous studies, large-scale triaxial apparatus has the capability of conducting cyclic load tests under controlled confining pressures. A large-scale triaxial apparatus (Indraratna et al. 1998) was used to conduct cyclic loading tests on RIBS specimens (300 mm diameter, 600 mm high) with different percentages of rubber (R_b=0-15%, by mass). The 0% of rubber content (R_b=0%) implies the conventional ballast material (latite basalt) was obtained from Bombo Quarry (New South Wales, Australia). Latite (volcanic) basalt is a crushed igneous rock aggregate and one of the primary sources of railway ballast used in the state of NSW, Australia. Its composition includes the minerals feldspar, plagioclase and augite, and more details of this ballast are given elsewhere (Indraratna et al. 1998). This selected ballast was sieved by a vibrating shaker using appropriate sieves and subsequently washed and dried as a clean ballast prior to testing. Rubber granules for the study were 100% recycled material supplied by Tyrecycle Australia. The amount of rubber in the testing samples is limited to 15% by mass because higher levels of rubber content can significantly compromise the stiffness of RIBS to cause unacceptable increase in settlement (Fathali et al. 2016; Sol-Sanchez et al. 2015; Esmaeili et al. 2016). To obtain a uniform mixture of RIBS for a given rubber content (R_b), precalculated weights of ballast particles and the dry rubber particles were mixed carefully in a cement mixer at a very slow rotating

speed (to avoid particle breakage). The maximum particle size of the mixture was 53mm to ensure that the ratio of the diameter of the test specimen (300 mm) to the largest particle size was approximately 6, to avoid the boundary effect. Figures 2(a-g) show the steps of specimen preparation and testing setup. Precalculated amount of material was divided into four portions and compacted with a rubber-padded vibrating plate inside the membrane in 150mm thick layers. Two split moulds were used to support the 7 mm thick membrane while preparing the specimen (Figs. 2 a-e). Figures 2(f-g) show the cylindrical outer cell chamber that houses the specimen, the vertical loading unit and the servo controller. Samples were prepared to the same initial void ratio of 0.824. After setting up the specimen, the test procedure included initial saturation, followed by the application of confining pressure and conditioning phase, and then cyclic loading. Then each sample was placed in the setup for 24 hours in fully saturated condition under the backpressure of 10 kPa until the Skempton's B value was more than 0.98. After setting up the apparatus, confining pressures ($\sigma_3' = 30$ and 60 kPa) were applied to the specimens and the pore water pressure was monitored throughout the tests to ensure effective drainage during cyclic loading. As notable initial settlement with increased rubber under static loading could be observed, at the outset of testing, a conditioning phase was introduced, where up to the maximum cyclic stress magnitude was applied monotonically to the test specimens before applying the cyclic loads at a frequency of 20 Hz. In addition to that, it minimises the effect of improper contact between the top and bottom ends of the specimen with the sample cap and base plate. This phenomenon is also comparable with the newly built tracks, in which trains are running at a slower speed at the beginning to ensure the track settles safely and reduce the chance of buckling. The details of the loading procedure are presented in Fig. 3. The loading frequency (*f*) was 20 Hz resembling train speed (v) of about 150 km/h (Hussaini et al. 2015). The maximum and the minimum cyclic deviator stress ($q_{cyc,max}$ and $q_{cyc,min}$) applied as a sinusoidal wave were 230 kPa and 45 kPa, respectively (Fig. 3). This is equivalent to 25 tonnes of axle load and in-situ stresses in the unloaded track (Lackenby et al. 2007). All the tests were conducted up to 400,000 cycles or until vertical deformation reached the limit of the equipment (@ 25% axial strain). Before and after the tests, the particles were sieved to quantify the ballast breakage according to the ballast breakage index (BBI) (Indraratna et al. 2005). The basic geotechnical properties (i.e., initial density, effective friction angle, and relative density) of RIBS are shown in Table 1. The maximum initial density (1535 kg/m^3) was for the pure ballast specimens while the minimum density of 1263 kg/m^3 was recorded for the RIBS specimens with R_b=15%. Also, the ballast friction angle was found to reduce slightly from 49° to 46° with the increase in R_b from 0 to 15%. This is in agreement with previous studies (e.g. Fathali et al. 2016), and this small reduction in friction angle is not of much concern as ballast aggregates having a friction angles even less than 45° is not uncommon. Moreover,

in the long term, the stiffness of the mixture may increase due to creep as reported by Tian and Senetakis (2021) that increases the contact area by compression and improved interlock between grains.

3. Test results and analysis

3.1 Void ratio

The void ratio, e of RIBS is calculated using the equation $e = \left(\frac{G_s \gamma_w}{\gamma_d}\right) - 1$, where G_s is the specific gravity of RIBS, γ_w is the unit weight of water, and γ_d is the dry unit weight. Here $\gamma_d = m_s/V$, where m_s is the mass of solids and V is the total volume. The specific gravity of RIBS (G_s) with different $R_b\%$ is calculated using the equation,

$$G_s = \frac{1}{\left(\frac{(1 - R_b\%)}{G_B}\right) + \frac{R_b\%}{G_R}} \quad (1)$$

where $G_B = 2.8$ and $G_R = 1.15$ are the specific gravity of ballast and rubber respectively. Figure 4 represents the void ratio (e) of the specimens at the beginning of the test (e_i), after the conditioning phase (e_0), and at the end of the test (e_f). It is obvious that, during the conditioning phase, the materials in all the samples are transformed to a denser granular assembly from the initial state, and the corresponding reduction in the void ratio is significant in relation to the increased rubber content. At the end of the tests, all the specimens have attained a void ratio, e_f in between 0.78-0.76 while the specimens after the conditioning phase (e_0) varies from 0.81-0.78. It was previously observed that under cyclic loading, granular material having a lower initial void ratio gave a smaller settlement than the granular material with a higher initial void ratio (Jeffs and Tew 1991; Selig and Waters 1994). Therefore, it is an advantage that the RIBS reach a lower void ratio under similar initial loading conditions (during the conditioning phase) and become more densified compared to the conventional ballast. Here the densification term is referred to irreversible rearrangement of grain configurations associated with the volumetric strain. In addition, permanent strains under initial loading conditions show a relatively similar performance as discussed in a previous study under monotonic loading (Arachchige et al. 2021).

3.2 Permanent deformation behavior

3.2.1 Axial strain

Figures 5(a-b) present the permanent axial strain with the number of cycles for the specimens subjected to the confining pressures of 30 and 60 kPa for different amounts of $R_b\%$. By the end of the cyclic loading the axial strain of RIBS with R_b=5% is slightly similar to that of pure ballast at σ'_3 =30 kPa, while the reductions in the axial strain for RIBS with R_b=10% and 15% are 23% and 65%, respectively. For a confining pressure of 60 kPa,

the reductions in the axial strain at the end of the test for R_b=10% and 15% are around 52% and 63% compared to the pure ballast. Also, an increase in confining pressure decreases the axial strains for all the samples irrespective of the rubber content. Unlike under monotonic loading, the axial strain response for long-term cyclic loading (> 400,000 cycles) elucidates an opposite effect indicating the lowest axial strains for samples with the highest rubber contents (R_b=15%). This is attributed to densification of the test specimens with higher rubber contents occurring quickly during initial loading, after which further cyclic loading does not cause significant compression. Moreover, reduced ballast degradation and increased damping property due to the higher rubber contents are also the reasons for the reduced deformation, and this will be discussed in the later sections.

The failure modes of specimens under drained stress-controlled cyclic loading are different from those of monotonic loading that occurs when the failure stress is exceeded. Werkmeister et al. (2005) reported a new shakedown mechanism to study the material deformation under repeated loads and later Sun et al. (2014) extended the idea of a shakedown mechanism for railway ballast. When progressively decreasing plastic axial strain rate eventually stabilises and leads to an asymptotic value in response to cyclic loading, the ballast achieves a state of 'plastic shakedown'. Pure ballast tested in the current study reached the plastic shakedown state by attaining a stable permanent deformation rate with the increased axial strain. This is in line with Sun et al. (2014) where pure ballast was tested under similar conditions to the current study (σ'_3 = 30 kPa, $q_{cyc\ max}$ = 230 kPa and frequency of 20 Hz). Figure 5 shows the permanent axial strain rate ($\delta\varepsilon_a/\delta N$) changing with the axial strain for the RIBS under σ'_3=30 and 60 kPa. From Fig. 4 it is clear that when R_b% increases, the permanent axial strain rate ($\delta\varepsilon_a/\delta N$) curves move clockwise indicating RIBS specimens progressively decreases to a fairly small plastic axial strain rate (up to around 10^{-8}) and attains a stable rate at a reduced axial strain. Hence the behaviour of RIBS also can be categorised into the plastic shakedown state irrespective of the rubber content. In design, the state of plastic shakedown is permitted, thus the risk of failure due to excessive settlements is lesser in RIBS compared to the conventional ballast subjected to similar conditions. The approximate points where the RIBS reach the plastic shakedown (no more accumulation of plastic strain) are marked in Figs. 5(c-d) as solid circles and corresponding approximate cycle numbers are indicated for each curve. It is clear that RIBS with $R_b \geq$10%, the rate of permanent axial deformation gradually reaches the plastic shakedown state after 200,000 cycles while for pure ballast and RIBS with R_b=5%, the rate of permanent axial deformation reaches the plastic shakedown after 50,000 cycles. This means attaining the plastic shakedown is delayed when the rubber content $R_b \geq$10%. Accumulation of plastic strain at a slower rate is preferred in practice to reduce track maintenance cycles which are required when the accumulated plastic deformation exceeds the tolerable limit.

3.2.2 Volumetric strain

As shown in Figs. 6(a-b), an increase of rubber in the RIBS reduces the volumetric strain against the number of cycles indicating that increased rubber in RIBS reduces the ballast dilation. The reason can be that the RIBS specimens undergo increased initial compression with increasing rubber contents during the conditioning phase, thus resulting in effective particle interlocking. This has already been observed in an earlier study by Arachchige et al. (2021), in which the tests have been conducted for RIBS under monotonic loading. As rubber particles are more compressible than rock aggregates, it is not surprising that the overall dilation of the granular mass is contained during the loading phase. As can be seen in Figs. 6(a-b), volumetric strain variation with the number of cycles (plotted in log scale) follows two distinct zones considering the slope of the curves. Zone A is the small-strain region where the volumetric strains are small (0-15% of total volumetric strain) and specimens are stable. After several loading cycles (i.e., N=1000 and N= 200 when the samples are subjected to 30 kPa and 60 kPa confining pressures respectively) the data plots in Zone A swiftly merge into quasi-concave shapes at larger strains as indicated by Zone B. With the increase of confining pressure, Zones A narrows down with a lesser number of cycles while Zone B becomes wider with the increased number of cycles. Figures 6(c-d) represent the rate of change in volumetric strain ($\delta\varepsilon_v/\delta N$) against the number of cycles that can differentiate these zones, where the curves are almost flat and stable in Zone A. At the beginning of Zone B, the data plots indicate a downward trend, and it is observed that the change in volumetric strain of Zone B decreases from around 10^{-5} to 10^{-9}. The volumetric strains at zone A (quasi-stable) are very small and can be neglected ($\varepsilon_v < 0.25\%$). Quasi-stable strains usually do not make an unfavourable effect on track deformations and passenger comfort. Therefore, Zone A is very sound in terms of stability. Zone B exhibits greater volumetric strain (dilation) levels and still tends to increase the volumetric strain even after 400,000 cycles. Therefore, Zone B is beyond the state of equilibrium; thus, it can cause considerable track instability. By mixing the ballast with granulated rubber, the volumetric strain in Zone B decreases significantly, hence increasing the stability of the track.

3.3 Resilient modulus

Resilient modulus (M_R) of ballast is a key parameter in railway design; it is an indication of the elastic response of granular material under repeated loads. M_R is defined as the ratio of the applied cyclic stress (Δq_{cyc}) to the recoverable strain (ε_{rec}), and the definition can be found in Fig. 7. Increased reversible deformation is one of the distinctive features of rubber, hence RIBS with increased rubber shows increased recoverable deformations in each cycle compared to the conventional ballast material. Therefore, as shown in Fig. 7, M_R decreases with the

increased content of R_b% in the RIBS (i.e., After around 100000 cycles M_R decreases approximately 25%, 40%, and 50% for RIBS with R_b=5%, 10%, and 15% respectively). Figures 6a and 6b show a slight increase of M_R for all the samples when the effective confining pressure is increased from 30 kPa to 60 kPa. A similar observation was also reported by (Indraratna et al. 2009; Hicks, 1970). This is because of the reduced particle sliding and rolling due to increased stress levels at the ballast contacts (Ngo et al. 2021). All the specimens are gradually densifying with the increased number of cycles, hence the M_R increases with the decreasing rate and tends to attain a stable value after around 100,000 cycles (Figs. 7 a-b). Generally the M_R of the pure ballast stabilises at a value of larger than 250 MPa when σ'_3> 30 and $q_{cyc,max}$ >230 kPa (Indraratna et al. 2009). Therefore, the increase of rubber content R_b>10% may not be acceptable for the use of RIBS in general tracks.

3.4 Damping ratio and energy dissipation capacity

The damping ratio, D, is an important parameter widely used in dynamic analysis to evaluate the efficiency of energy dissipation for granular materials. As shown in Figs. 8(a-b), the damping ratio can be computed by the equation, $D = \frac{A_L}{4\pi A_T}$ where A_L is the area enclosed by the hysteresis loop and A_T is the area of the triangle. Here, the loop area $A_L$is the measure of dissipated energy per unit volume during a cycle (E_d), and triangle area A_T represents the stored elastic energy (Madhusudhan et al. 2017). The energy dissipated per cycle (E_d) against the cycle number (N) is shown in Figs. 8(c-d). An increase in rubber content in the RIBS increases the damping ratio as well as the energy dissipation, and the damping ratio of all the specimens attains a stable stage after around 100,000 cycles. The nature of the rubber is highly elastic and that mainly contributes to the increased damping properties of RIBS with increased rubber contents. The damping ratios of RIBS are larger than that of pure ballast because the elasticity of rubber granules facilitates the rearrangement of particles and relative movements. Therefore, increased energy dissipation is observed for RIBS with $R_b \geq$5%. Figures 6(a-d) show that no distinctive increase can be observed for damping ratio and energy dissipation when R_b>10%. The reason can be that the increased rubber content in the RIBS ultimately leads to a more rubber-like material that deviates from the behaviour of an unbonded granular medium. In other words, R_b=15% can be considered the threshold beyond which the material behaviour is more pronouncedly controlled by the rubber granules. However, an increase in confining pressure decreases the damping ratio and energy dissipation. Increased confining pressures relatively reduce the particle movement in granular media due to the increased interparticle friction hence the dissipated energy reduces. Moreover, increased rubber content surpasses the effect of confining pressure (Fig. 8a-b); hence compared to pure ballast (R_b=0%), the reduction of damping ratio of RIBS due to the increased confining pressure

is reduced. This is because the increasing rubber-to-rubber and/or rubber-to-ballast interfaces reduce the component of rigid particle contacts, hence reducing the plasticity and irrecoverable compression. This is particularly so when the host material is ballast that has a rougher surface texture compared to finer-grained soil particles (e.g. uniform sand) (Senetakis et al. 2012; Tian et al. 2021).

3.5 Ballast degradation

Considering the importance of quantifying the ballast breakage, Indraratna et al. (2005) introduced a method specifically for ballast material to evaluate the particle breakage, namely Ballast Breakage Index (BBI). Ballast Breakage Index or BBI is a significant modification of the relative breakage index (Hardin, 1985). BBI is specifically formulated for the relatively narrow hence uniform range of railway ballast (typically 10-55 mm, with a corresponding uniformity coefficient < 2; Indraratna et al. 2011), for which the horizontal scale for grain sizes can be conveniently represented using an arithmetic scale. In this approach, the value of BBI is conveniently quantified by the area ratio subtended by the shift in the ballast gradation curve at a given time considering an arbitrary lower limit for fine gravel, i.e., > 2.36mm sieve (Fig. 9). In contrast, Hardin's approach considers a very broad particle size distribution, thereby adopting a logarithmic horizontal scale for the grain sizes, for which the lower bound is taken as the 74-micron sieve capturing coarse silt to fine sand. In this respect, Hardin's method is not practical for most real-life conditions of ballast degradation; this is because, under typical heavy haul loading and routine track maintenance conditions, the degraded ballast aggregates still fall within the gravel range, as realistically incorporated in the BBI approach. Figure 9 shows that the increase of rubber content in the RIBS mixture up to 5% considerably decreases the BBI (43% and 23% reduction in BBI under the confining pressures of 60 kPa and 30 kPa respectively), but a further reduction of BBI is insignificant when the rubber content increases from 5% to 10% (17% and 7% further reduction under the confining pressures of 60 kPa and 30 kPa respectively). Again, the addition of 5% rubber (R_b=15%), provides a considerable reduction in BBI. Therefore, the pattern of particle breakage can be characterised by three distinct degradation zones: (i) $R_b \leq 5\%$: rubber particles predominantly act as a void filler, thus reducing abrasion between ballast particles with a notable reduction in ballast breakage; (ii) 5%< R_b <10%: ballast breakage is less sensitive to the variation of rubber content, as the initial small amount of R_b= 5% had already fulfilled much of its role as a void filler within the fabric of RIBS; (iii) R_b>10%: rubber particles replace a significant fraction of the breakable ballast particles apart from void filling, thus enabling a significant reduction in BBI. Figure 9 also shows the ballast degradation patterns observed during testing, and they can be classified into three categories: (a) angular corner breakage or abrasion,

(b) grinding or wearing away from the surface or attrition, and (c) splitting into two or more equal particles. This is in agreement with previous studies on ballast e.g. Lees and Kennedy (1975); Qi and Indraratna (2020).

4 Discussion

Laboratory tests reveal that RIBS enhances the ballast performance generally but at the same time slightly compromises some of the important properties (i.e., stiffness, initial settlements and resilient modulus) to some extent. Therefore, particular attention needs to be taken when selecting the rubber content in RIBS that optimises the ballast performance. In the RIBS material, there is a trend of increasing the initial settlements during the conditioning phase by the compressibility of rubber particles, but it is possible that sufficient compaction and tamping can avoid any undue initial settlement to an admissible limit. The reduced particle breakage and effective particle interlocking during the conditioning phase can make RIBS less compressible compared to a standard ballasted track. The rubber content R_b=5% in RIBS would not make a significant difference in reducing the axial and volumetric strains under cyclic loads, whereas $R_b \geq 10\%$ can make a significant impact on reducing the long-term ballast deformation.

Attaining the shakedown state makes the material stiffer as there is no more plastic deformation in terms of grain breakage and creep of the rubber particles. Following the mechanism suggested by Tian and Senetakis (2021), it is clear that the deformation due to the increased grain breakage is expected to be prominent in pure ballast, whereas rubber-induced creep deformations can dominate the plastic deformation in RIBS. In other words, creep influence on RIBS may further increase both performance and longevity of track.

It is known through past studies that the energy dissipation capacity of RIBS increases with the rubber content, as the granular assembly becomes more ductile with the increased value of R_b%. For instance, specimens of RIBS having 5% rubber can double the energy dissipation capacity compared to the conventional ballast material, and 10 % rubber performs even better by enhancing almost twice the capacity of 5% RIBS (Fig. 8c-d). Further increase in rubber (R_b=15%) does not make a significant contribution to the energy dissipation capacity compared to the RIBS with 10% rubber, and it further reduces the resilient modulus. In other words, increasing R_b>10% reduces the resilient modulus M_R less than 250 MPa which is generally the minimum recorded for the pure ballast from many studies (Indraratna et al. 2009).

As discussed earlier, increasing the rubber content up to 15%, not only fills the voids but also replaces some of the breakable ballast particles with rubber, and these particles may contribute to a more uniform contact force distribution. In this case, a higher rubber content (i.e., 15%) may reduce the shear strength of the ballast layer,

where significantly reduced peak deviator stresses were observed for similar specimens with R_b=15% under monotonic loads. Therefore, RIBS with increased rubber (R_b >10%) may not be practical for the tracks that are subjected to increased axle loads (>25 tonnes).

In essence, under cyclic loads, it is clear that RIBS with R_b=10% demonstrates improved performance as an alternative ballast material as the optimum rubber content. As also identified in this study, compared to pure ballast, RIBS densifies more under similar initial loading conditions and thereby ensures less settlements during the subsequent application of cyclic loading. Increased compaction is required for pure ballast to achieve a much more reduced void ratio similar to the RIBS material ($R_b \geq$5%) and that can cause increased ballast breakage. Therefore, the RIBS can be considered expedient in terms of compaction under the same loading while assuring less ballast breakage.

Aursudkij (2007) identified that tamping tine insertion is another main source of ballast degradation. RIBS makes the particle interfaces softer hence, it would reduce the ballast breakage during the tamping compared to the conventional ballast. Moreover, the drainage potential is one of the other major concerns of using RIBS material in real tracks. During testing, even at the lowest void ratio (when the rubber granules are compressed most), the observed excess pore water pressures were found to be negligible. Compared to the impervious membrane used in the triaxial specimen, the surrounding boundary of RIBS would not be covered in real tracks. This implies that any infiltrated water can be drained even more effectively than during laboratory tests. However, due to the lightweight of the rubber granules, there is a possibility of washing away the rubber particles during a flood or heavy rainfall. In this case, for the locations that are susceptible to waterlogging, conventional ballast material can be used as the crib ballast while RIBS are only placed below the sleeper load-bearing layer.

5 Conclusion

Large-scale cyclic triaxial tests were conducted to investigate the dynamic properties of RIBS with varying rubber content (0-15% by mass) and associated behaviour under cyclic loading (i.e., deformation, resilient modulus, damping ratio, ballast breakage) subjected to different confining pressures (30 and 60 kPa) under a loading frequency of 20 Hz. The following conclusions can be drawn based on the test results.

1. This study confirms that during the conditioning phase (strain controlled static loading up to the maximum cyclic stress), RIBS attains a denser granular assembly attributed to the compression of rubber granules, i.e. resulting in a reduced void ratio. Compared to pure ballast ($R_b = 0\%$), the reduction in void ratio of RIBS test specimens is in the proximity of 3, 4 and 5 times for R_b =5, 10 and 15%,

respectively. This densification contributed to reducing the permanent axial strains by 23 to 65% corresponding to increasing values of R_b (10 to 15%) and confining pressure (30 to 60 kPa).

2. Although all test specimens reached plastic shakedown at an axial strain between 1% and 3%, the addition of rubber delayed the specimens attaining shakedown (At N≈ 50,000 for pure ballast and N≈200,000 for RIBS with $R_b = 10\%$). From a practical perspective, by reaching the state of plastic shakedown at a reduced axial strain in comparison with pure ballast, RIBS is clearly beneficial in making the track maintenance cycles less frequent and cost-effective.

3. The addition of the rubber and the increase in confining pressure reduced the volumetric strain (dilation) of RIBS specimens, which could be categorised into two distinct zones, namely, Zone A (quasi-stable) at small strains and Zone B at subsequent larger volumetric strains corresponding to a greater number of loading cycles. This leads to the conclusion that ballast tracks may compromise stability in the long run (Zone B), but the addition of even a small percentage of rubber in RIBS to contain excessive volumetric strain (dilation) can be considered as an obvious benefit.

4. An increase in rubber content in RIBS increased the corresponding damping ratio and the energy absorption capacity. For example, 10% of rubber almost doubled the damping ratio and increased the energy dissipation capacity by approximately three times that of pure ballast, while sustaining an adequate resilient modulus (> 250 MPa) for the RIBS material.

5. Under the confining pressure of 30 kPa ballast breakage of RIBS was decreased by approximately 25%, 30% and 80% with the increase in rubber content by 5, 10, and 15%, respectively. The role of rubber particles within RIBS could be identified as threefold: (i) predominantly void filling ($R_b \leq 5\%$), (ii) fulfilling the role of void filling to an optimum volume within the RIBS fabric ($5\% < R_b \leq 10\%$), and (iii) unbreakable rubber crumbs replacing an equivalent fraction of breakable ballast particles, apart from void filling ($10\% < R_b \leq 15\%$).

As a final note, through this laboratory work, RIBS epitomised its potential as an appropriate blending material for ballast for reducing track deformation and particle breakage under cyclic loading. The test results demonstrated that 10% by weight of rubber could be considered as the optimum rubber content to be used in RIBS, as a further increase in rubber content would generate diminishing economic returns in relation to track maintenance.

Funding

The research leading to these results received funding from Australian Research Council Linkage Project (ARC-LP200200915) and ARC Industry Transformation Training Centre for Advanced Rail Track Technologies (ITTC-Rail IC170100006).

Declaration of Competing Interest

The authors declare that they have no known competing financial interests or personal relationships that could have appeared to influence the work reported in this paper.

Acknowledgments

The authors would like to acknowledge the financial assistance provided by the Australian Research Council Linkage Project (ARC-LP200200915) and ARC Industry Transformation Training Centre for Advanced Rail Track Technologies (ITTC-Rail IC170100006). The financial and technical assistance provided by industry partners including Bridgestone and Australasian Centre for Rail Innovation (ACRI), is gratefully acknowledged.

Data Availability Statement

Some or all data, models, or code generated or used during the study are available from the corresponding author by request (cyclic triaxial test data).

References

1. Arachchige, C. M. K., Indraratna, B**.,** Qi, Y., Vinod, J. S., and Rujikiatkamjorn, C. (2021). "Geotechnical characteristics of a Rubber Intermixed Ballast System". *Acta Geotechnica*., 1-12. https://doi.org/10.1007/s11440-021-01342-2
2. AREMA. (2010). Manual for railway engineering, Vol. 1: Track, Ch. 1: Roadway and ballast. American Railroad Engineering and Maintenance of Way Association (AREMA), Washington, D.C.
3. AS (Australian Standards), (2015). "Aggregates and rock for engineering purposes. Part 7: Railway ballast." *AS 2758.7,*Standards Australia.
4. Aursudkij, B. (2007). "A laboratory study of railway ballast behaviour under traffic loading and tamping maintenance." Doctoral dissertation, Univ. of Nottingham, England.
5. DEQ. (1989). *Rhinehart tire fire dum*. Virginia Department of Environmental Quality, Winchester, 1-3.

6. Tyre Stewardship Australia. (2020). *Used tyres supply chain and fate analysis*. Randell Environmental Consulting Pty Ltd. Victria, Australia.

7. Esmaeili, M., Ebrahimi, H., and Sameni, M. K. (2018). "Experimental and numerical investigation of the dynamic behavior of ballasted track containing ballast mixed with TDA." *Proc., Inst. Mech. Eng. Part F: J. Rail Rapid Transit.,* 232 (1), 297–314. https://doi.org/10.1177/ 0954409716664937

8. Esmaeili, M., Zakeri, J. A., Ebrahimi, H., and Sameni, M. K. (2016). "Experimental study on dynamic properties of railway ballast mixed with tire derived aggregate by modal shaker test." *Adv. Mech. Eng.,* 8 (5), 1687814016640245. https://doi.org/10.1177/1687814016640245

9. Fathali, M., Nejad, F. M., and Esmaeili, M. (2016). "Influence of tire-derived aggregates on the properties of railway ballast material." *J. Mater. Civ. Eng.*, 29 (1). https://doi.org/10.1061/(ASCE)MT.1943-5533.0001702

10. Gong, H., Song, W., Huang, B., Shu, X., Han, B., Wu, H., and Zou, J. (2019). "Direct shear properties of railway ballast mixed with tire derived aggregates: Experimental and numerical investigations." *Constr. Build. Mater.,* 200 (Mar), 465–473. https://doi.org/10.1016/j.conbuildmat.2018.11.284

11. Hardin, B.O., (1985). "Crushing of soil particles." *J. Geotech. Eng.*, 111(10), 1177-1192. https://doi.org/10.1061/(ASCE)0733-9410(1985)111:10(1177)

12. Hicks, R. G. 1970. "Factors influencing the resilient properties of granular materials." Doctoral dissertation, Univ. of California, Berkeley, California.

13. Hussaini, S. K. K., Indraratna, B., and Vinod, J. S. (2015). "Performance assessment of geogrid-reinforced railroad ballast during cyclic loading." *Transp. Geotech.,* 2, 99–107. https://doi.org/10.1016/j.trgeo.2014.11.002

14. Indraratna, B., Ionescu, D., and Christie, H. D. (1998). "Shear behaviour of railway ballast on large-scale triaxial tests." *J. Geotech. Geoenviron. Eng.*, 124(5), 439-449. https://doi.org/10.1061/(ASCE)1090-0241(1998)124:5(439)

15. Indraratna, B., Lackenby, J., and Christie, D. (2005). "Effect of confining pressure on the degradation of ballast under cyclic loading." *Géotechnique,* 55(4), 325–328. https://doi.org/10.1680/geot.2005.55.4.325

16. Indraratna, B., Salim, W., and Rajikiatkamjorn, C. (2011). "Advanced rail geotechnology: Ballasted track." CRC Press, Rotterdam, Netherlands.

17. Indraratna, B., Vinod, J. S., and Lackenby, J. (2009). "Influence of particle breakage on the resilient modulus of railway ballast." *Géotechnique,* 59(7), 643–646. https://doi.org/10.1680/geot.2008.T.005

18. Jayasuriya, C., Indraratna, B., and Ngo, T. N. (2019). "Experimental study to examine the role of under sleeper pads for improved performance of ballast under cyclic loading." *Transp. Geotech.*, 19, 61-73. https://doi.org/10.1016/j.trgeo.2019.01.005

19. Jeffs, T., and Tew, G. (1991). *A Review of Track Design Procedures–Volume 2: Sleepers and Ballast.* Railways of Australia, Australia.

20. Kim, H. K. and Santamarina, J. C. (2008). "Sand–rubber mixtures (large rubber chips)." *Can. Geotech. J.*, 45(10), 1457-1466. https://doi.org/10.1139/T08-070

21. Koohmishi, M. and Azarhoosh, A. (2020). "Hydraulic conductivity of fresh railway ballast mixed with crumb rubber considering size and percentage of crumb rubber as well as aggregate gradation." *Constr. Build. Mater.*, 241, 118133. https://doi.org/10.1016/j.conbuildmat.2020.118133

22. Koohmishi, M. and Azarhoosh, A. (2021). "Degradation of crumb rubber modified railway ballast under impact loading considering aggregate gradation and rubber siz." *Can. Geotech. J.*, 58, 398-410. https://doi.org/10.1139/cgj-2019-0596

23. Lackenby, J., Indraratna, B., Mcdowell, G., and Christie, D. (2007). "Effect of confining pressure on ballast degradation and deformation under cyclic triaxial loading." *Géotechnique,* 57(6), 527-536. https://doi.org/10.1680/geot.2007.57.6.527

24. Lee, J.S., Dodds, J. and Santamarina, J. C. (2007). "Behavior of rigid-soft particle mixtures." *J. mater. Civ. Eng.,* 19, 179-184. https://doi.org/10.1061/(ASCE)0899-1561(2007)19:2(179)

25. Lees, G. and Kennedy, C. K. (1975). "Quality, shape and degradation of aggregates." *Q. J. Eng. Geol.*, 8, 193-209. https://doi.org/10.1144/GSL.QJEG.1975.008.03.03

26. Madhusudhan, B., Boominathan, A. and Banerjee, S. (2017). "Static and large-strain dynamic properties of sand–rubber tire shred mixtures." *J. Mater. Civ. Eng*, 29, 04017165. https://doi.org/10.1061/(ASCE)MT.1943-5533.0002016

27. Navaratnarajah, S. K., Indraratna, B. and Ngo, N. T. (2018). "Influence of under sleeper pads on ballast behavior under cyclic loading: experimental and numerical studies." *J. Geotech. Geoenviron. Eng.*, 144(9). https://doi.org/10.1061/(ASCE)GT.1943-5606.0001669

28. Ngo, T., Indraratna, B. and Ferreira, F. (2021). "Influence of synthetic inclusions on the degradation and deformation of ballast under heavy-haul cyclic loading." *Int. J. Rail Transp,* 1-23. https://doi.org/10.1080/23248378.2021.1964390

29. Perez, J. L., Kwok, C. and Senetakis, K. (2016). "Effect of rubber size on the behaviour of sand-rubber mixtures: A numerical investigation." *Comput. Geotech*., 80, 199-214. https://doi.org/10.1016/j.compgeo.2016.07.005

30. Qi, Y. and Indraratna, B. (2020). "Energy-based approach to assess the performance of a granular matrix consisting of recycled rubber, steel-furnace slag, and coal wash." *J. Mater. Civ. Eng*, 32, 04020169. https://doi.org/10.1061/(ASCE)MT.1943-5533.0003239

31. Qi, Y., and Indraratna, B. (2021). "The influence of rubber inclusion on the dynamic response of rail track." *J. Mater. Civ. Eng*, 34(2), 04021432. https://doi.org/10.1061/(ASCE)MT.1943-5533.0004069

32. Remennikov, A., Kaewunruen, S., and Ikaunieks, K. (2006). "Deterioration of dynamic rail pad characteristics." *Proc., Conf. on Railway Engineering,* Melbourne, Australia.

33. Selig, E. T., and Waters, J. M. (1994). *Track technology and substructure management,* Thomas Telford, London.

34. Senetakis, K., Anastasiadis, A. and Pitilakis, K. (2012). "Dynamic properties of dry sand/rubber (SRM) and gravel/rubber (GRM) mixtures in a wide range of shearing strain amplitudes." *Soil Dyn. Earthq. Eng,* 33, 38-53. https://doi.org/10.1016/j.soildyn.2011.10.003

35. Sidhu, K.S., Keeslar, F.L. and Warner, P.O. (2006). "Potential health risks related to tire fire smoke." *Toxicol. Int*, 13(1), 1-17.

36. Sol-sánchez, M., Moreno-navarro, F., and Rubio-gámez, M. (2014). "The use ofdeconstructed tires as elastic elements in railway tracks." *Materials,* 7, 5903-5919. https://doi.org/10.3390/ma7085903

37. Sol-Sanchez, M., Moreno-Navarro, F., and Rubio-Gámez, M. C. (2015). "A study into the use of crumb rubber in railway ballast." *Constr. Build. Mater*., 75, 19-24. https://doi.org/10.1016/j.conbuildmat.2014.10.045

38. Song, W., Huang, B., Shu, X., Wu, H., Gong, H., Han, B., and Zou, J. (2019). "Improving damping properties of railway ballast by addition of tire-derived aggregate." *Transp. Res. Rec.*, 2673, 299-307. https://doi.org/10.1177/0361198119839345

39. Sun, Q., Indraratna, B., and Nimbalkar, S. (2014). “Effect of cyclic loading frequency on the permanent deformation and degradation of railway ballast.” *Géotechnique,* 64, 746-751. https://doi.org/10.1680/geot.14.T.015

40. Tawk, M., Qi, Y., Indraratna, B., Rujikiatkamjorn, C., and Heitor, A. (2021). “Behavior of a Mixture of Coal Wash and Rubber Crumbs under Cyclic Loading.” *J. Mater. Civ. Eng.,* 33, 04021054. https://doi.org/10.1061/(ASCE)MT.1943-5533.0003667

41. Tian, Y., Kasyap, S. S. and Senetakis, K. (2021). “Influence of loading history and soil type on the normal contact behavior of natural sand grain-elastomer composite interfaces.” *Polymers,* 13, 1830. https://doi.org/10.3390/polym13111830

42. Tian, Y. and Senetakis, K. (2021). “Influence of creep on the small-strain stiffness of sand–rubber mixtures.” *Geotechnique*, 1-12. https://doi.org/10.1680/jgeot.20.P.208

43. Thakur, P.K., Vinod, J.S. and Indraratna, B., (2013). “Effect of confining pressure and frequency on the deformation of ballast”. *Géotechnique*, *63*(9), 786-790. https://doi.org/10.1680/geot.12.T.001

44. Werkmeister, S., Dawson, A. R., and Wellner, F., (2005). “Permanent deformation behaviour of granular materials.” *Road. Mater. Pavement Des.,* 6(1), 31–51. https://doi.org/10.1080/14680629.2005.9689998

List of tables

Table 1. Basic properties of RIBS

R_b (%) in the RIBS mixture (% by weight)	Rubber content (% by volume)	Initial density (kg/m^3)	Relative density, Dr %	Effective friction angle, φ_{ef}
0	0	1535	1.00	48.8
5	6.2	1432	0.93	48.4
10	11.7	1342	0.87	47.7
15	16.5	1263	0.82	46

List of figures

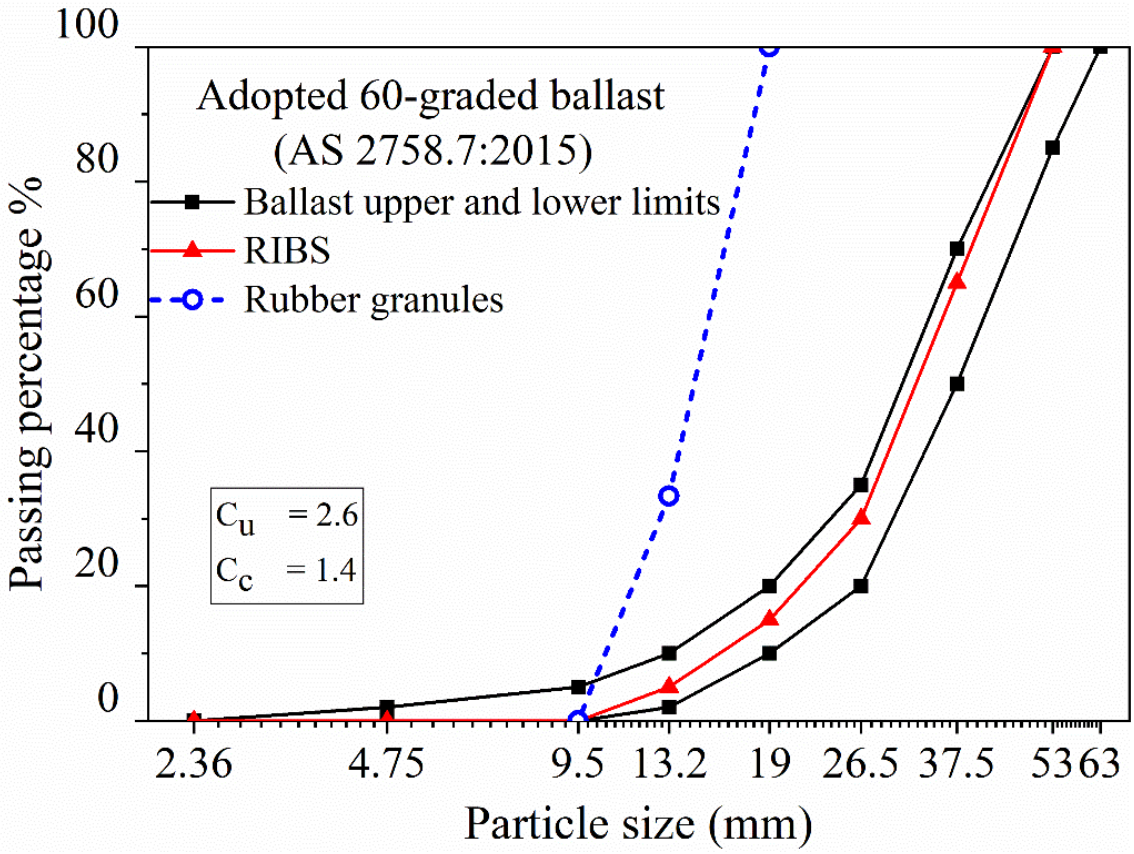

Fig.1. Particle size distribution of RIBS and rubber granules

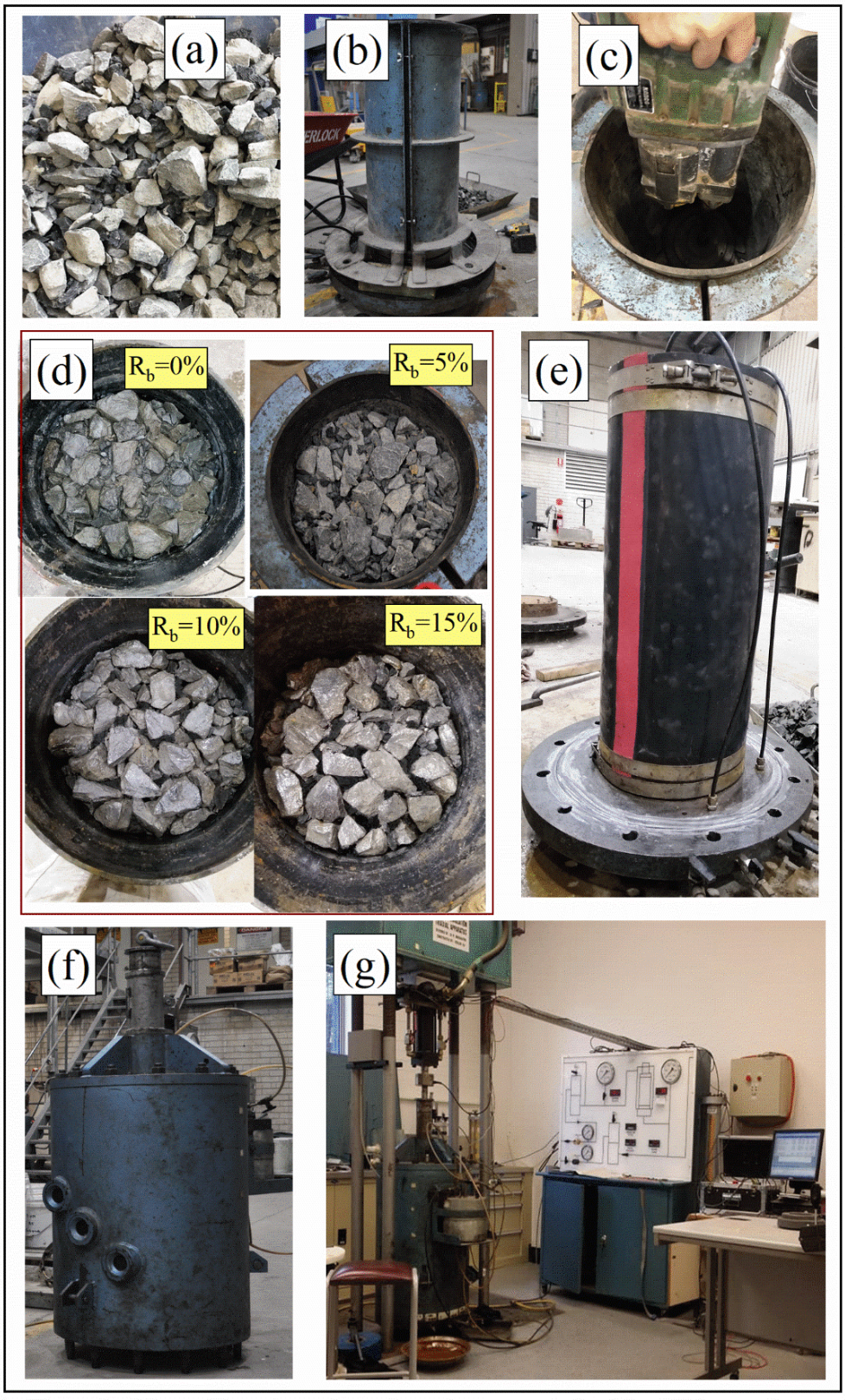

Fig.2. Sample preparation and test setup: (a) prepared RIBS material (R_b=5%); (b) 7mm membrane supported by two split moulds; (c) layer compaction with a vibrating plate; (d) last

layer of RIBS (R_b=0-15%); (e) prepared sample; (f) sample is placed inside the outer cell chamber; (g) setup of the large scale triaxial apparatus

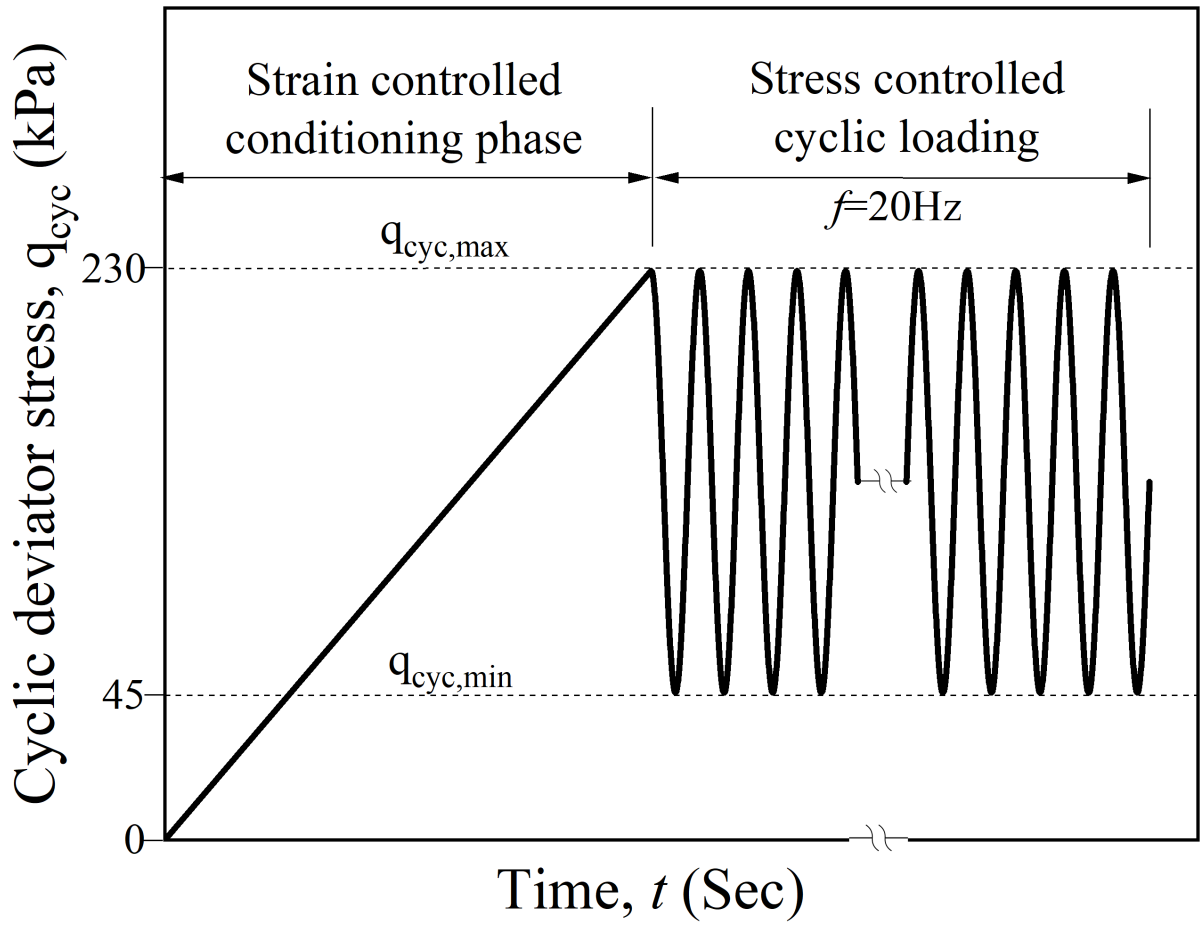

Fig. 3. Details of the loading procedure

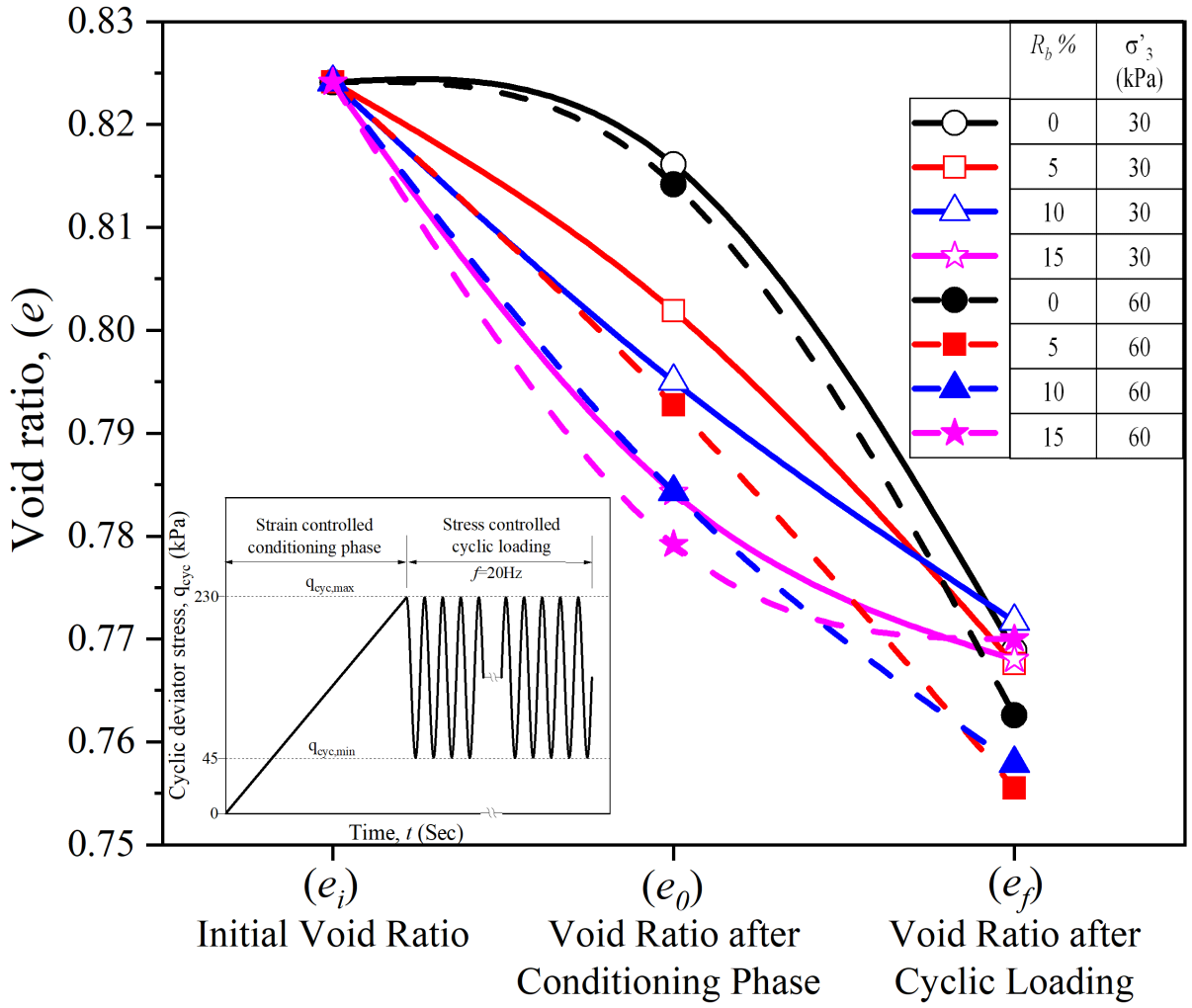

Fig. 4. Void ratio (e) of the specimens at the beginning of the test (e_i), after the conditioning phase (e_0) and at the end of the test (e_f)

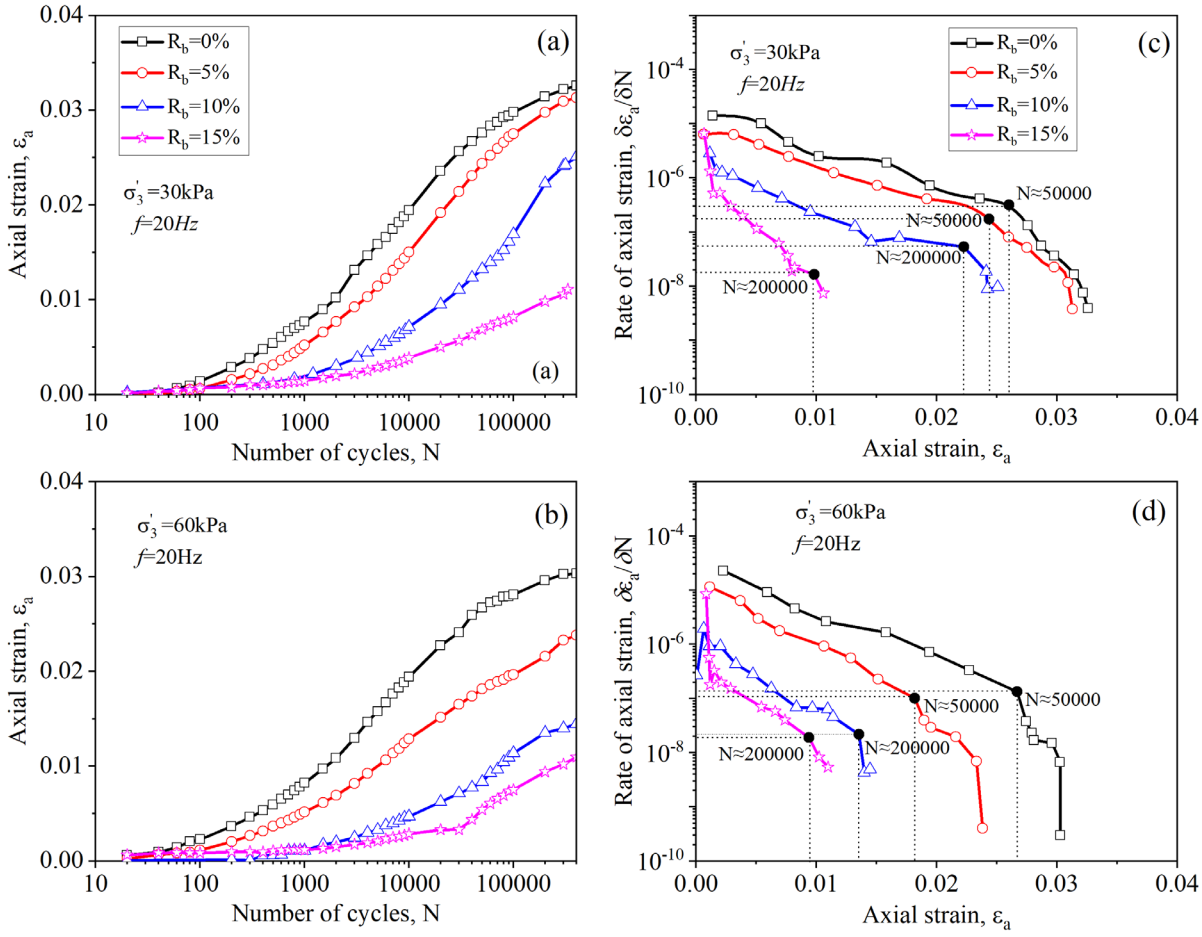

Fig.5. (a-b) Axial strain response of RIBS mixtures under effective confining pressures: (a) 30 kPa (b) 60 kPa; **(c-d)** rate of axial strain variation of RIBS mixtures under effective confining pressures: (c) 30 kPa (d) 60 kPa

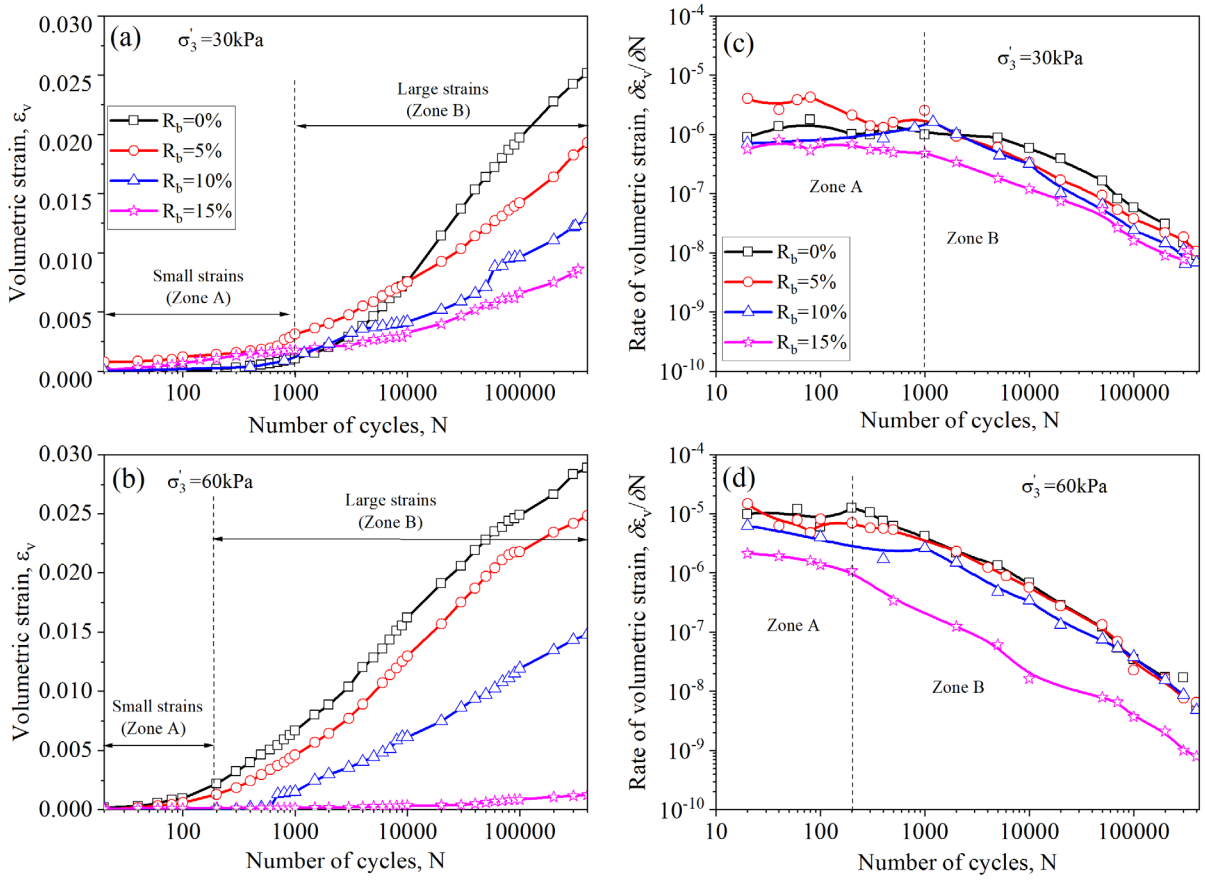

Fig. 6. (a-b) Volumetric strains (dilation) of RIBS mixtures under effective confining pressures: (a) 30 kPa (b) 60 kPa; **(c-d)** volumetric strain rates with respect to number of cycles under effective confining pressures: (c) 30 kPa (d) 60 kPa

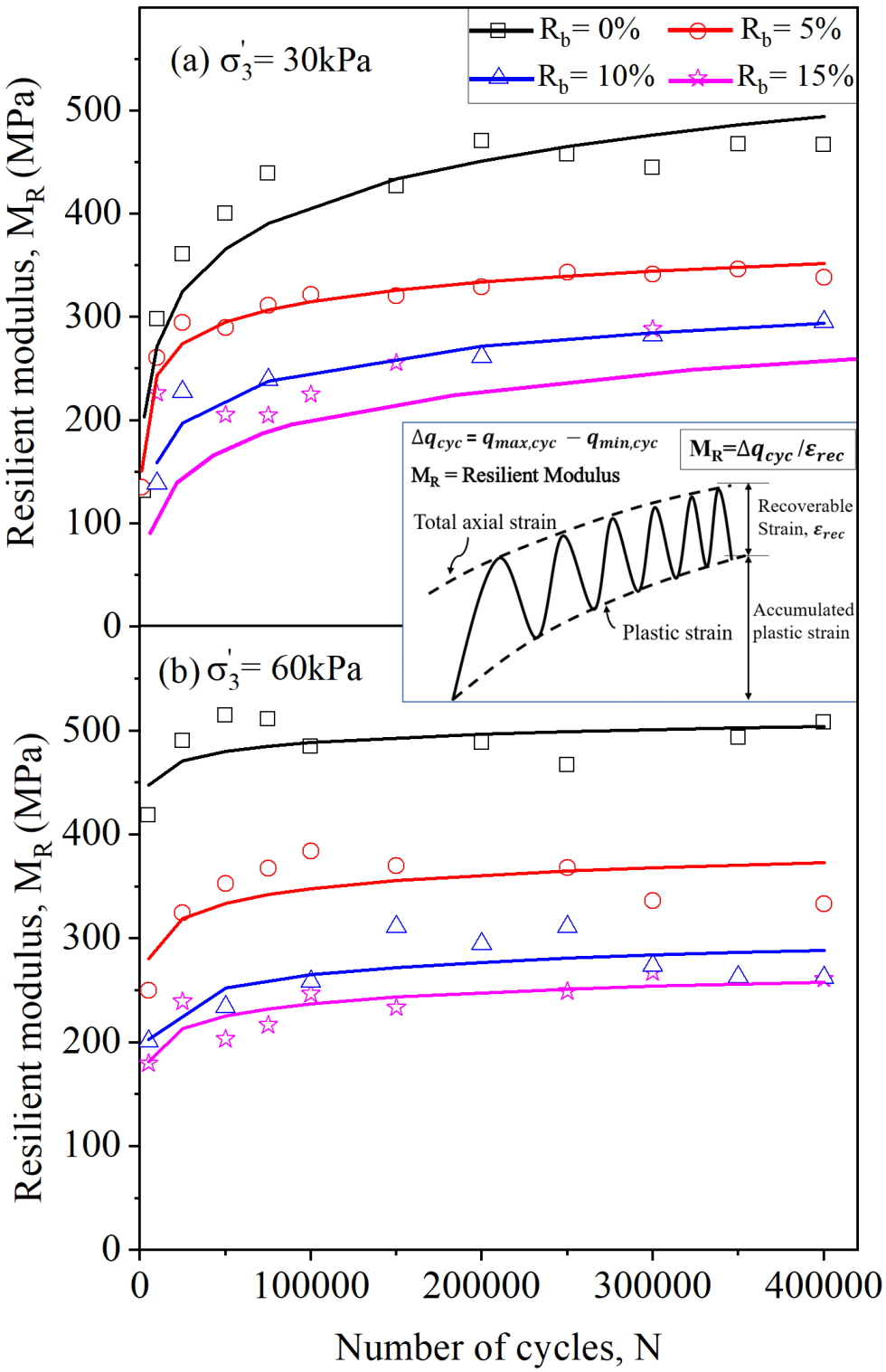

Fig. 7. Variation of resilient modulus of RIBS mixtures against the number of cycles under effective confining pressures: (a) 30 kPa (b) 60 kPa

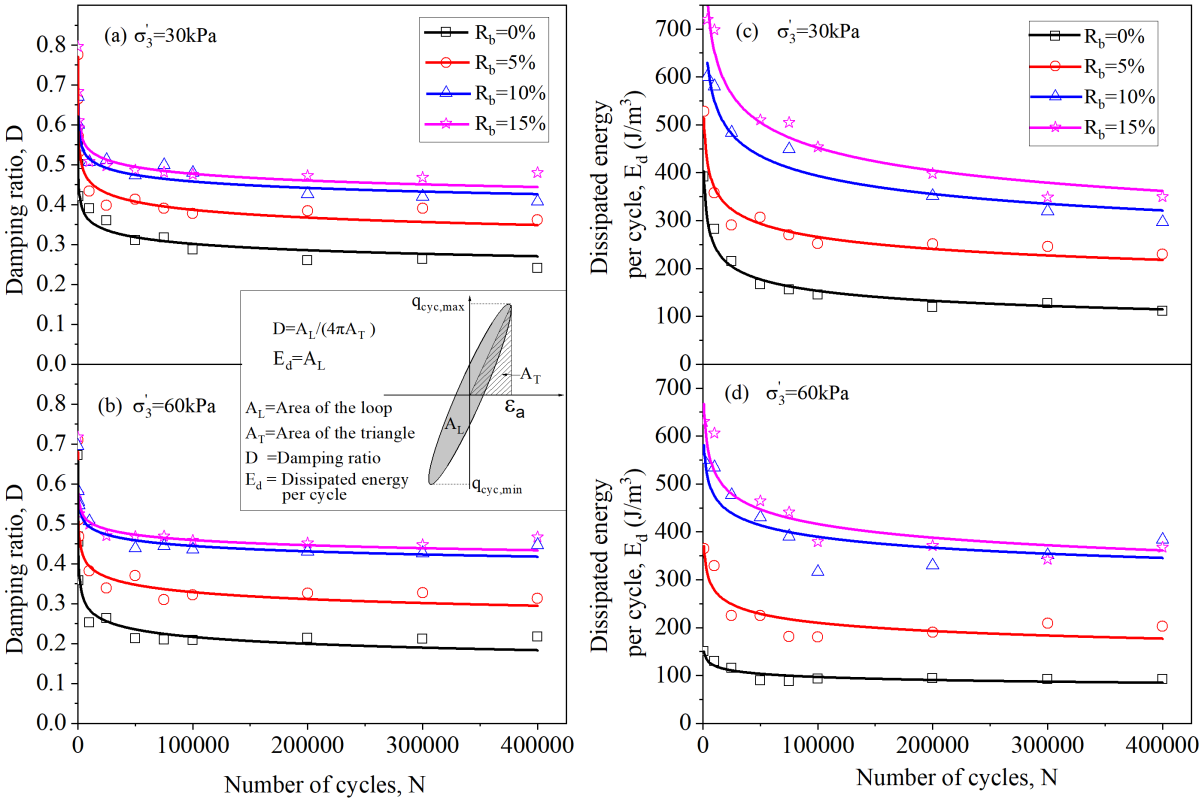

Fig. 8. (a-b) Variation of damping ratio against the number of cycles under effective confining pressures: (a) 30 kPa, (b) 60 kPa; **(c-d)** variation of dissipation energy against the number of cycles under effective confining pressures: (c) 30 kPa, (d) 60 kPa

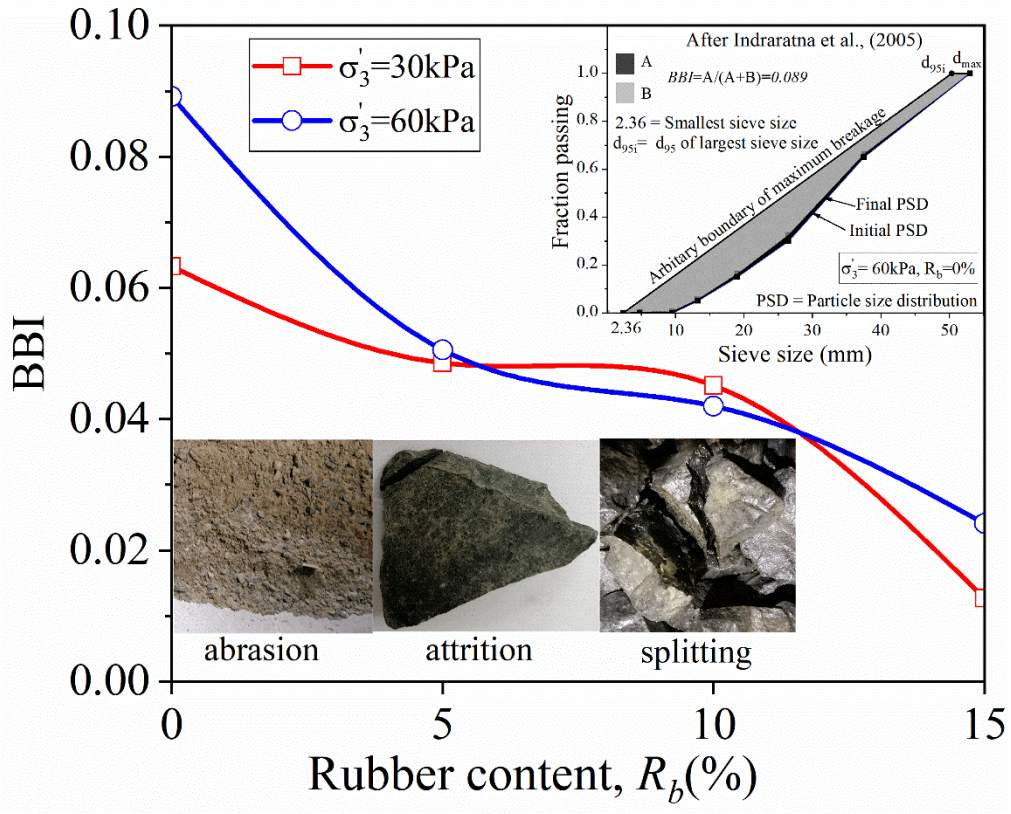

Fig. 9. Influence of R_b on Ballast Breakage Index, BBI